GGAs: A Family of ADP Ribosylation Factor-binding Proteins Related to Adaptors and Associated with the Golgi Complex✪

Esteban C. Dell'Angelica, Rosa Puertollano, Chris Mullins, Rubén C. Aguilar, José D. Vargas, Lisa M. Hartnell, and Juan S. Bonifacino

Cell Biology and Metabolism Branch, National Institute of Child Health and Human Development, National Institutes of Health, Bethesda, Maryland 20892

Abstract. Formation of intracellular transport intermediates and selection of cargo molecules are mediated by protein coats associated with the cytosolic face of membranes. Here, we describe a novel family of ubiquitous coat proteins termed GGAs, which includes three members in humans and two in yeast. GGAs have a modular structure consisting of a VHS domain, a region of homology termed GAT, a linker segment, and a region with homology to the ear domain of γ-adaptins. Immunofluorescence microscopy showed colocalization of GGAs with Golgi markers, whereas immunoelectron microscopy of GGA3 revealed its presence on coated vesicles and buds in the area of the TGN. Treatment with brefeldin A or overexpression of dominant-negative ADP ribosylation factor 1 (ARF1) caused dissociation of GGAs from membranes. The GAT region of GGA3 was found to: target a reporter protein to the Golgi complex; induce dissociation from membranes of ARF-regulated coats such as AP-1, AP-3, AP-4, and COPI upon overexpression; and interact with activated ARF1. Disruption of both *GGA* genes in yeast resulted in impaired trafficking of carboxypeptidase Y to the vacuole. These observations suggest that GGAs are components of ARF-regulated coats that mediate protein trafficking at the TGN.

Key words: trans-Golgi network • ADP ribosylation factor • coats • adaptins • VHS

Introduction

Protein trafficking at various stages of the endocytic and secretory pathways is mediated by vesicular intermediates that carry cargo molecules between different membrane-bound compartments. Both the formation of these intermediates and cargo selection depend upon the function of a set of protein coats that are recruited from the cytosol to membranes (reviewed by Mellman, 1996; Rothman and Wieland, 1996; Schekman and Orci, 1996; Kirchhausen et al., 1997). Some coats contain as their key constituents either one of four heterotetrameric adaptor protein (AP)[1] complexes (subunit compositions indicated in parentheses): AP-1 (γ-β1-μ1-σ1); AP-2 (α-β2-μ2-σ2); AP-3 (δ-β3-μ3-σ3); or AP-4 (ϵ-β4-μ4-σ4; reviewed by Hirst and Robinson, 1998; Bonifacino and Dell'Angelica, 1999; Kirchhausen, 1999). AP-2 has the shape of a "head" with two protruding "ears" (Heuser and Keen, 1988); the other three complexes are thought to have a similar structure. A more distantly related coat protein complex, known as coatomer or COPI (α-β-β′-γ-δ-ϵ-ζ), has been shown to play a role in ER–Golgi and endocytic trafficking pathways (reviewed by Lippincott-Schwartz et al., 1998; Wieland and Harter, 1999).

Recruitment of AP-1, AP-3, AP-4, and COPI, but not AP-2, from the cytosol to membranes is regulated by members of the ADP-ribosylation factor (ARF) family of small GTP-binding proteins (Donaldson et al., 1992a,b; Robinson and Kreis, 1992; Palmer et al., 1993; Stamnes and Rothman, 1993; Traub et al., 1993; Faundez et al., 1998; Ooi et al., 1998; Dell'Angelica et al., 1999a; Hirst et al., 1999). ARF1 is the most abundant member of the family and also the most active for recruitment of COPI and AP-3 to membranes (Liang and Kornfeld, 1997; Ooi et al., 1998); other ARFs (ARF2-5) may also be able to regulate

✪The online version of this article contains supplemental material.

Address correspondence to Juan S. Bonifacino, Cell Biology and Metabolism Branch, National Institute of Child Health and Human Development, Building 18T, Room 101, National Institutes of Health, Bethesda, MD 20892. Tel.: (301) 496-6368. Fax: (301) 402-0078. E-mail: juan@helix.nih.gov

[1]*Abbreviations used in this paper:* 3AT, 3-amino-1,2,4-triazole; AP, adaptor protein; ARF, ADP-ribosylation factor; BFA, brefeldin A; CPY, carboxypeptidase Y; GAE, γ-adaptin ear; GAL4ad, GAL4 transcription activation domain; GAL4bd, GAL4 binding domain; GAT, GGA and TOM1; GFP, green fluorescent protein; GST, glutathione-S-transferase; GTPγS, guanosine 5′-O-(3-thiotriphosphate); ORF, open reading frame; TOM1, target of myb1.

coat recruitment. In contrast, ARF6 does not seem to play a role in coat recruitment (Peters et al., 1995; Ooi et al., 1998), but rather in remodeling the plasma membrane and underlying actin cytoskeleton (Radhakrishna et al., 1996). Like other GTP-binding proteins, ARFs cycle between GDP-bound (inactive) and GTP-bound (active) forms, which are localized to the cytosol and membranes, respectively (reviewed by Boman and Kahn, 1995; Moss and Vaughan, 1998). Membrane-bound ARF1-GTP has been shown to be the species that promotes recruitment of COPI onto membranes (Donaldson et al., 1992a), either directly by interacting with the coat proteins themselves (Zhao et al., 1997), or indirectly through local modification of the lipid composition of the membranes (Ktistakis et al., 1996).

Although it is now well established that AP complexes, COPI and ARFs play key roles in the molecular mechanisms responsible for vesicle formation and cargo selection, it is also clear that they constitute only part of the coat-mediated trafficking machinery. Here we report the identification of a novel family of adaptor-related proteins referred to as GGAs (for Golgi-localized, γ ear-containing ARF-binding proteins), which are ubiquitously expressed in mammalian and yeast cells. The three mammalian and two yeast GGA proteins have a modular structure consisting of (in NH_2- to COOH-terminal order): a VHS domain (Lohi and Lehto, 1998); a region of homology termed GAT; a linker segment; and a domain with homology to the ear of the γ1-adaptin subunit of AP-1 and the related γ2-adaptin. The mammalian GGAs are components of coats that are mainly associated with the TGN in an ARF-dependent manner. The GAT region mediates both targeting to the Golgi complex and interaction with activated ARF1. Overexpression of constructs having the GAT region causes dissociation of ARF1-regulated coats from membranes. Finally, disruption of genes encoding the two yeast GGA homologues impairs sorting of carboxypeptidase Y (CPY) to the vacuole, consistent with a role of these proteins in biosynthetic protein transport. All of these observations suggest that GGAs are components of the molecular machinery that mediates protein trafficking at the TGN.

Materials and Methods

Nucleic Acid Manipulations

A cDNA segment comprising codon 5 to the stop codon of the long form of human GGA1 was PCR-amplified from a human heart cDNA library, using primers based on partial genomic DNA sequences from GenBank/EMBL/DDBJ (accession numbers AL035496.6 and Z83844). The 5′ primer included an additional sequence to place a Myc epitope at the protein's NH_2 terminus. The first codons and a short 5′ untranslated region were obtained from the same cDNA library by 5′RACE-PCR. The complete open reading frame (ORF) of human GGA2 was PCR-amplified from a human pancreas cDNA library using primers that were designed based on the sequence of the A-735G6.4 gene (GenBank/EMBL/DDBJ accession number AC002400). The ORFs encoding long and short forms of GGA3 were isolated by a combination of PCR and 5′RACE-PCR, using for primer design the sequence of the DNA clone KIAA0154 (GenBank/EMBL/DDBJ accession number D63876). All the above PCR products were cloned into the pCR 3.1 vector (Invitrogen) and sequenced.

The construct GST-$GGA2_{GAE}$ was generated by PCR amplification of codons 424–613 of human GGA2 and subsequent cloning into the BamHI–NotI sites of the pGEX-5X-1 vector (Pharmacia Biotech). The constructs GST-$GGA3_{VHS}$, GST-$GGA3_{VHS\text{-}GAT}$, and GST-$GGA3_{GAE}$ were obtained by PCR amplification of codons 1–146, 1–313, and 494–723 of the human GGA3 long isoform, respectively, followed by cloning into the EcoRI–NotI sites of the pGEX-5X-1 vector. GFP-fusion constructs, comprising different regions of the GGA3 long isoform, were prepared by PCR and subsequent cloning into the EcoRI–SalI sites of the pEGFP-C2-MCS vector (Clontech), as follows: GFP-VHS (residues 1–146); GFP-VHS-GAT (residues 1–313); and GFP-GAT (residues 147–313). The inserts of these three constructs were subcloned into the pGAD424 vector to generate analogous two-hybrid constructs. Additional constructs prepared in the pGAD424 two-hybrid vector by PCR and in-frame cloning were as follows: residues 1–352 of GGA3 long isoform ($GGA3_{VHS\text{-}GAT\text{-}39}$; EcoRI–SalI); residues 494–723 of GGA3 long isoform ($GGA3_{GAE}$; EcoRI–BglII); residues 5–247 of human GGA1 ($GGA1_{VHS\text{-}GAT}$; EcoRI–SalI); and residues 1–330 of human GGA2 ($GGA2_{VHS\text{-}GAT}$; EcoRI–SalI). The insert of the two-hybrid construct $GGA3_{GAE}$ was subcloned into the EcoRI–BamHI sites of the pEGFP-C2-MCS vector to generate the GFP-GAE construct. The two-hybrid ARF1/Q71L construct was engineered by PCR from the HA-ARF1-Q71L mammalian expression plasmid (Ooi et al., 1998) and cloned in-frame (without the HA sequence) into the EcoRI–XhoI sites of the pGBT9 vector (Clontech). The corresponding two-hybrid ARF1/T31N plasmid and the GST-γ2-$adaptin_{GAE}$ construct were kindly provided by Chean Eng Ooi (National Institutes of Health, Bethesda, MD).

Antibodies

Polyclonal antibodies to human GGA2 and GGA3 were raised in rabbits using as immunogens purified GST-$GGA2_{GAE}$ and GST-$GGA3_{GAE}$, respectively. Both antibodies were affinity-purified on columns containing their corresponding immunogens coupled to Affi-Gel 15 (BioRad). Rabbit polyclonal antibody to human TGN46 was a gift from Vas Ponnambalam (University of Dundee, UK). Antibodies to yeast CPY were gifts of Tom Stevens (University of Oregon, Eugene, OR) and Carol Woolford (Carnegie Mellon University, Pittsburgh, PA). The following antibodies were purchased from the providers indicated in parentheses: HA.11 mAb to the HA epitope and 9E10 mAb to the Myc epitope (Berkeley Antibody Co.); mAb to 58-K Golgi protein (Sigma Chemical Co.); rabbit anti–β-COP and 1D9 monoclonal anti-ARF (Affinity Bioreagents); rabbit anti-Rab4 (Santa Cruz); mouse monoclonal anti-dynamin I (Transduction Laboratories); sheep anti–human TGN46 (Serotec); and rabbit anti–sheep IgG (Jackson ImmunoResearch Laboratories). The sources of the remaining antibodies have been indicated in previous reports (Dell'Angelica et al., 1999a,b).

Cell Culture and General Biochemical Procedures

The sources and culture conditions of the human cell lines HeLa, M1, H4, Jurkat, Caco-2, MEG-01, and MNT-1 have been described previously (Dell'Angelica et al., 2000). Metabolic labeling of cells in culture with [^{35}S]methionine, preparation of Triton X-100 and detergent-free extracts, salt extraction of postnuclear membranes, ultracentrifugation on sucrose gradients, and immunoprecipitation–recapture were carried out as described previously (Dell'Angelica et al., 1997). Recombinant GST-fusion proteins were purified by using glutathione-Sepharose 4B beads (Pharmacia Biotech).

Transfection and Immunofluorescence

Transfection of HeLa cells was performed by using FuGENE-6 (Roche Molecular Biochemicals). Immunofluorescence microscopy analysis was carried out as described (Dell'Angelica et al., 1999a). Images were acquired on Zeiss LSM 410 or LSM 510 confocal microscopes. The lack of antibody cross-reactivity or optical cross-over on two-color fluorescence experiments was corroborated using appropriate controls done in parallel.

Immunoelectron Microscopy

Immunoelectron microscopy of ultrathin frozen sections of HeLa cells transfected with a GGA3 construct was performed essentially as described (Slot and Geuze, 1983). In brief, cells were fixed in 4% formaldehyde, 0.1 M phosphate buffer (pH 7.4) for 2 h at room temperature, scraped, and embedded in 10% gelatin. Gelatin blocks were incubated for 16 h in 2.3 M sucrose at 4°C, and then frozen in liquid nitrogen. Ultrathin frozen sections were made with a cryoultramicrotome (Reichert Ultracut S) and transferred to grids using sucrose/methyl cellulose droplets. Sec-

tions were treated with 1% fish skin gelatin and 0.15 M glycine before incubation at room temperature with rabbit antibody to GGA3. Bound antibody was detected by incubation with protein A conjugated to 5-nm (for double-labeling) or 10-nm (for single-labeling) gold particles (Utrecht University, The Netherlands). For double-labeling experiments, sections were subsequently incubated with sheep anti–human TGN46, rabbit anti–sheep IgG, and then 10-nm protein A-gold. Labeled sections were examined with a Philips CM 10 transmission electron microscope.

Yeast Two-Hybrid Assays

The *Saccharomyces cerevisiae* strain HF7c was transformed by the lithium acetate procedure as described in the instructions for the MATCHMAKER two-hybrid kit (Clontech). For colony growth assays, two colonies of each HF7c transformant were resuspended in water to 0.1 $O.D_{600}$/ml, then 5 μl were applied on plates lacking leucine and tryptophan, or leucine, tryptophan and histidine, and allowed to grow at 30°C for 3–4 d. β-galactosidase assays of HF7c transformants were done by using the colony-lift filter assay (Clontech).

In Vitro ARF-binding Assays

Purified recombinant ARF1/Q71L (kindly provided by Paul Randazzo, NIH) was activated by incubating for 1 h at 32°C in binding buffer (25 mM Hepes, pH 7.4, 0.1 M NaCl, 1 mM dithiothreitol, 1 mM EDTA, 1 mM $MgCl_2$, 0.5 g/liter BSA, 0.1% w/v Triton X-100) containing 0.1 mM guanosine 5′-O-(3-thiotriphosphate) (GTPγS). A control incubation in buffer lacking GTPγS was carried out in parallel. Bovine brain cytosol (9 mg/ml) was similarly incubated in binding buffer containing protease inhibitors [1 mM 4-(2-aminoethyl)-benzenesulfonyl fluoride, 10 mg/liter aprotinin, 2 mg/liter leupeptin, 1 mg/liter pepstatin A], in the presence or absence of 0.1 mM GTPγS. Following the incubation period, samples were centrifuged for 5 min at 100 *g* and further incubated with glutathione-Sepharose 4B beads containing 20 μg of GST-fusion proteins, either at room temperature for 30 min (for recombinant ARF1/Q71L) or at 4°C for 1 h (for bovine brain cytosol). Beads were subsequently washed twice with ice-cold binding buffer and once with ice-cold binding buffer lacking Triton X-100. Bound proteins were analyzed by immunoblotting.

Disruption of Yeast GGA1 and GGA2 Genes and Pulse–Chase Analysis of CPY Processing

DNA fragments comprising ~480 bp upstream of the start codon to nucleotide number 570 of the yeast *GGA1* ORF (YDR358w) and ~200 bp upstream of the start codon to the stop codon of the yeast *GGA2* ORF (YHR108w) were amplified by PCR from yeast genomic DNA and cloned into pCR2.1 (Invitrogen). To create the *GGA1* disruption cassette, an 823-bp fragment containing the *TRP1* gene and its promoter was amplified from plasmid yDp-W (Berben et al., 1991) using 5′ and 3′ primers engineered to contain SacII restriction sites. This fragment was cloned into the SacII site (*GGA1* ORF nucleotide 46) of the *GGA1* genomic clone. To create the *GGA2* disruption cassette, a 1.15-kb fragment containing the *HIS3* gene and its promoter was amplified from plasmid yDp-H (Berben et al., 1991) using 5′ and 3′ primers engineered to contain BstEII and ClaI restriction sites, respectively. The *GGA2* genomic clone was digested with BstEII and ClaI to remove 1,024 bp of the *GGA2* ORF and allow insertion of the *HIS3* marker. Fragments consisting of the *GGA1* genomic sequence containing the *TRP1* marker and the *GGA2* genomic sequence containing the *HIS3* marker were then transformed individually and in combination into wild-type haploid yeast strain SEY6210 (Herman and Emr, 1990). Homologous recombinants were selected on minimal media lacking the appropriate amino acid(s). Putative disruption strains were then screened by PCR and verified by Southern blot analysis. Pulse–chase analysis of yeast strains with [^{35}S]methionine (Mullins et al., 1995), immunoprecipitation with CPY antiserum (Hampton and Rine, 1994) and secretion of CPY (Roberts et al., 1991) were performed as described.

Online Supplemental Materials

The online version of this article includes figures that accompany the information presented here and is available at http://www.jcb.org/cgi/content/full/149/1/81/DC1.

Supplemental Figure 1. Multiple sequence alignments of VHS (A), GAT (B), and GAE (C) regions of human GGAs and the corresponding segments of related human proteins. γ1, γ1-adaptin; γ2, γ2-adaptin. GenBank/EMBL/DDBJ accession numbers are indicated in the legend to Fig. 1. The positions of the segments within the proteins' primary structures are indicated by residue numbers next to the sequences. Highlighted letters represent residues conserved in at least four (A) or three (B and C) of the proteins.

Supplemental Figure 2. Intracellular localization of Myc-GGA1 and GGA2 analyzed by indirect immunofluorescence microscopy of transfected cells. HeLa cells transfected with either Myc-GGA1 (A–C, G–I) or both GGA2 and HA-tagged TGN38 (D–F) were fixed, permeabilized, and stained as follows: A–C, mouse antibody to the Myc epitope and rabbit antibody to TGN46 followed by Alexa-488–conjugated donkey anti–mouse IgG (A and C, green channel) and Cy3-conjugated donkey anti–rabbit IgG (B and C, red channel); D–F, rabbit antibody to GGA2 and mouse antibody to the HA epitope followed by Cy3-conjugated donkey anti-rabbit IgG (D and F, red channel) and Alexa-488–conjugated donkey anti-mouse IgG (E and F, green channel); and G–I, mouse antibody to the Myc epitope and rabbit antibody to GGA3 followed by Alexa-488–conjugated donkey anti–mouse IgG (G and I, green channel) and Cy3-conjugated donkey anti–rabbit IgG (H and I, red channel). Stained cells were examined by confocal fluorescence microscopy. Bar, 10 μm.

Results

Identification and Domain Organization of GGA Proteins

Homology searches of sequences derived from both genomic and EST sequencing projects revealed the existence of at least three novel human genes encoding proteins with similarity to the ear domain of the γ1-adaptin subunit of AP-1. The complete ORFs of these proteins, herein referred to as GGA1 (GenBank/EMBL/DDBJ accession number AF218584), GGA2 (GenBank/EMBL/DDBJ accession number AC002400) and GGA3 (GenBank/EMBL/DDBJ accession numbers AF219138 and AF219139 for long and short alternatively spliced forms, respectively), were isolated from human cDNA libraries using a combination of PCR and 5′ RACE. Complete or partial sequences of GGA2 and GGA3 (short isoform) recently have been published by others as a result of large-scale DNA sequencing projects (Nagase et al., 1995; Kikuno et al., 1999; Loftus et al., 1999). The GGAs have also been independently identified by Boman et al. (2000) and Hirst et al. (2000). Northern blot analyses have shown that the three human GGA mRNAs are expressed in all human tissues examined (our unpublished observations; see also Nagase et al., 1995; Kikuno et al., 1999). Subsequent database searches revealed the occurrence of GGA-related proteins in other eukaryotic organisms. In particular, two ORFs from *S. cerevisiae*, YDR358w and YHR108w, were deemed to encode the yeast counterparts of human GGAs; we refer to these proteins as yeast Gga1p and Gga2p, respectively.

The three human and two yeast GGAs were found to share a similar domain organization consisting of four distinct regions (Fig. 1; and Supplemental Figure 1, http://www.jcb.org/cgi/content/full/149/1/81/DC1). The first region, comprising ~140 residues proximal to the GGAs' NH_2 termini, displays significant homology to the VHS domain, a protein module previously found in the vertebrate proteins TOM1 (i.e., target of myb 1; not to be confused with mitochondrial outer membrane proteins), TOM1L1, Hrs, Hrs-2, and STAM1, as well as in yeast Vps27p (Lohi and Lehto, 1998, and references therein). The second region, comprising the next ~160 residues, is highly homologous among the human GGAs and contains

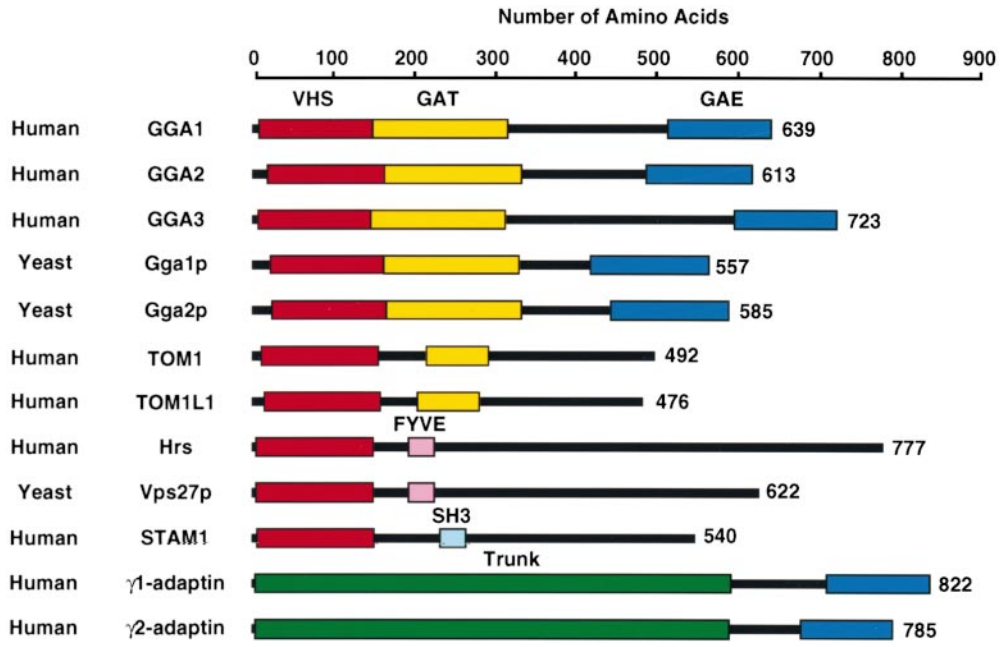

Figure 1. Schematic representation of GGAs and related proteins. Total numbers of amino acid residues of each protein are noted on the right. Specific domains or regions of homology are color coded. Black lines denote variable regions with no significant homology. Accession numbers are as follows: human GGA1, AF218584; human GGA2 (A-735G6.4), AC002400; human GGA3 (long isoform), AF219138; yeast Gga1p (YDR358w), NC_001136; yeast Gga2p (YHR108w), NC_001140; human TOM1, AJ006973; human TOM1-L1, AJ010071; human Hrs, D84064; yeast Vps27p, U24218; human STAM1, U43899; human γ1-adaptin, AB015317; human γ2-adaptin, AB015318.

an ~85 residue segment with low but significant homology to human TOM1 and TOM1L1. We refer to this region as "GAT" to denote the occurrence of homology among the GGA and TOM1 proteins. The GAT region has a high propensity to fold into coiled coil structures. The third region is much less conserved among the GGAs; it is of variable size, rich in prolines and serines, and predicted to adopt a random coil conformation. Finally, the ~125 residues proximal to the GGAs COOH termini display significant homology to the ear domains of the γ1-adaptin subunit of mammalian AP-1 and of the closely related γ2-adaptin protein (Robinson, 1990; Lewin et al., 1998; Takatsu et al., 1998). We refer to this region as GAE, for γ-adaptin ear homology domain.

Biochemical Characterization of Endogenous GGA2 and GGA3 in Human Cells

To study the biochemical properties of the human GGAs, we raised polyclonal antibodies to GST-fusion proteins bearing the corresponding GAE domains. Antibodies to GGA2 and GGA3 allowed us to identify the endogenous proteins in HeLa cells, by using an immunoprecipitation–recapture procedure (Fig. 2 A). The electrophoretic mobility of the protein recognized by the anti-GGA2 antibody corresponded to a polypeptide of ~70 kD, a molecular mass that was in close agreement with that predicted for human GGA2 (67.2 kD). The apparent molecular mass of the protein isolated with the antibody to GGA3 (~90 kD) was larger than that expected for the long isoform of GGA3 (78.3 kD). However, specificity controls convinced us that the ~90-kD protein corresponded to GGA3. First, the protein was isolated only when the anti-GGA3 antibody was used in both the first and second immunoprecipitation steps (Fig. 2 A). Second, recognition of this protein by the anti-GGA3 antibody was completely inhibited by excess GST-$GGA3_{GAE}$, but not by similar amounts of GST or GST-$GGA2_{GAE}$ (data not shown). Finally, the anti-GGA3 antibody did not crossreact with endogenous GGA2, the γ1-adaptin subunit of AP-1, or overexpressed Myc-GGA1 (data not shown). Both GGA2 and GGA3 were expressed in a wide variety of human cell lines (Fig. 2 B), in agreement with the results of Northern blot analyses.

Subcellular fractionation of metabolically labeled HeLa cells yielded most of endogenous GGA2 and GGA3 in a cytosolic fraction. A small (<10%) fraction, however, was associated with a postnuclear membrane pellet (Fig. 2 C). The membrane-associated forms of both GGA2 and GGA3 could be extracted with 0.2 M sodium carbonate, pH 11 (data not shown). These results suggested that GGA2 and GGA3 exist as both soluble and peripherally membrane-bound forms.

To estimate the sizes of the soluble forms of GGA2 and GGA3, a cytosolic extract was fractionated by ultracentrifugation on a 5–20% sucrose gradient, and the resulting fractions were analyzed by immunoprecipitation–recapture (Fig. 2 D). Both GGA2 and GGA3 were recovered from fractions corresponding to a sedimentation coefficient of ~3.5 S. This value was significantly smaller than those obtained for heterotetrameric AP complexes (e.g., 10 S for AP-4; Dell'Angelica et al., 1999a), thus suggesting that GGA2 and GGA3 are not components of AP-like complexes. Rather, the calculated sedimentation coefficients of GGA2 and GGA3 are more compatible with these proteins existing as monomers or dimers with an asymmetric shape. GGA2 did not coprecipitate with GGA3 (Fig. 2 A) or GGA1 (Hirst et al., 2000), suggesting that they do not form stable dimers with one another.

Localization of GGAs to the Golgi Complex and Peripheral Cytoplasmic Structures

To examine the intracellular localization of the human GGA proteins, we initially performed indirect immunofluorescence microscopy analysis on fixed-permeabilized HeLa cells using the rabbit polyclonal antibodies to the

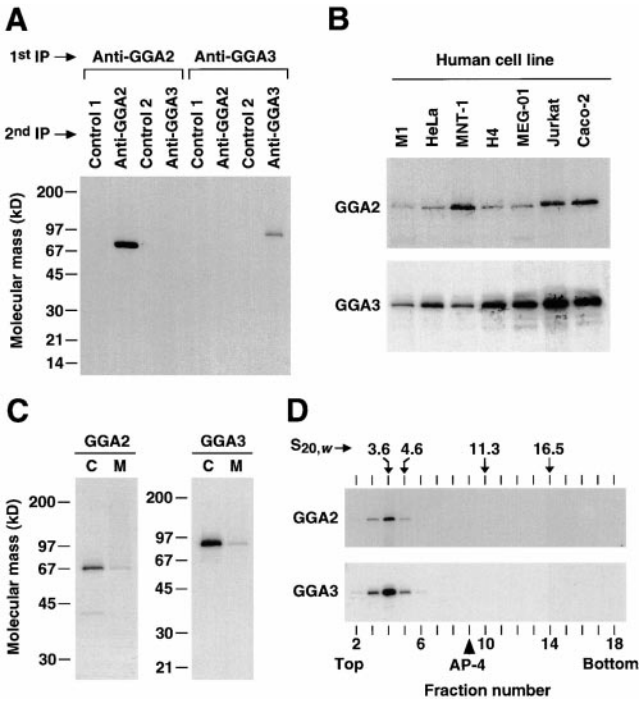

Figure 2. Biochemical characterization of endogenous GGA2 and GGA3. A, HeLa cells were metabolically labeled with [^{35}S]methionine for ~22 h and lysed in the presence of Triton X-100 (Dell'Angelica et al., 1997). The cleared extract was immunoprecipitated using antibodies to GGA2 or GGA3, and the resulting precipitates were subjected to a second immunoprecipitation step using antibodies to GGA2, GGA3, or two irrelevant proteins. The final immunoprecipitates were analyzed by 4–20% SDS-PAGE and fluorography. B, The indicated human cell lines were labeled with [^{35}S]methionine and subjected to immunoprecipitation–recapture, using antibodies to GGA2 (top) or GGA3 (bottom). C, A detergent-free extract (Dell'Angelica et al., 1997) of metabolically labeled HeLa cells was centrifuged first at 600 *g* for 5 min to remove nuclei and then at 120,000 *g* for 90 min to obtain cytosolic (C) and post-nuclear membrane (M) fractions. Both fractions were subjected to immunoprecipitation–recapture with antibodies to GGA2 or GGA3. D, A cytosolic fraction obtained as in C was loaded onto a 4–20% sucrose gradient and centrifuged in an SW-41 Beckman rotor at 39,000 rpm for 17 h at 4°C. Collected fractions were analyzed for GGA2 and GGA3 by immunoprecipitation–recapture. The positions of protein standards and the AP-4 complex in the gradient are indicated by arrows and an arrowhead, respectively.

GAE domains of GGA2 and GGA3. Only the antibody to GGA3 was found to detect the endogenous antigen under these conditions (Fig. 3). This antibody gave punctate staining of a juxtanuclear structure resembling the Golgi complex (Fig. 3, A, D, G, J, M, and P). Staining was judged to be specific, as it could be inhibited by addition of a GST-GGA3$_{GAE}$ fusion protein (Fig. 3 B) but not by GST-GGA2$_{GAE}$ (Fig. 3 C), GST-γ2-adaptin$_{GAE}$ (data not shown) or GST (Fig. 3 A).

The juxtanuclear structure stained by the anti-GGA3 antibody displayed partial colocalization with the TGN markers, TGN38 (Fig. 3, D–F) and furin (Fig. 3, G–I), and, to a lesser extent, with the cis-medial Golgi marker, 58-K protein (Fig. 3, J–L). We also observed partial colocalization of GGA3 with AP-1 in the juxtanuclear area of the cell, although the patterns of staining were not coincident (Fig. 3, M–O). There was little colocalization of GGA3 with AP-3 in the area of the Golgi complex (Fig. 3, P–R, left inset). However, we could observe faint staining for GGA3 in peripheral cytoplasmic foci, some of which did colocalize with AP-3 (Fig. 3, P–R, right inset), as well as with AP-1 (data not shown). We did not detect any colocalization of GGA3 with the plasma membrane-associated AP-2 complex (data not shown). Taken together, these observations suggest that GGA3 is mainly associated with the TGN, with an additional population of molecules localized to a peripheral cytoplasmic compartment.

Myc-epitope-tagged GGA1 (Myc-GGA1) or untagged GGA2 expressed at moderate levels by transfection into HeLa cells also exhibited good colocalization with TGN markers (Supplemental Figure 2, http://www.jcb.org/cgi/content/full/149/1/81/DC1). In addition, Myc-GGA1 colocalized with endogenous GGA3 (Supplemental Figure 2, http://www.jcb.org/cgi/content/full/149/1/81/DC1). Similar observations were made for endogenous GGA1 and epitope-tagged GGA2 by Hirst et al. (2000). These observations suggest that, like GGA3, GGA1 and GGA2 are predominantly localized to the TGN.

Association of GGA3 with Coated Membranes in the Area of the TGN

The intracellular localization of human GGA proteins was further investigated by immunoelectron microscopy on ultrathin HeLa cell sections. As labeling of endogenous GGA3 yielded a very low signal, we expressed higher levels of the untagged protein by transfection. Staining of cells expressing moderate levels of the transgene with anti-GGA3 antibody revealed specific labeling in an area of tubules and vesicles adjacent to the Golgi stack (Fig. 4 A). A more detailed inspection of structures stained for GGA3 revealed that the gold particles were associated with budding membrane profiles covered with an electron-dense coat (Fig. 4 B). The region labeled for GGA3 was identified as the TGN by double-labeling with anti-GGA3 and anti-TGN46 antibodies (Fig. 4 C). Similar analyses performed on HeLa cells transfected with Myc-GGA1 also showed concentration of label in the area of the TGN, although significant labeling of the Golgi stack was also observed (data not shown).

Regulation of GGA Localization by ARFs

Since ARF1 regulates recruitment of various protein coats to membranes, it was of interest to investigate whether this was also the case for GGAs. To this end, we first examined the effect of treating HeLa cells with brefeldin A (BFA), a pharmacological inhibitor of ARF1 guanine nucleotide exchange activity (Donaldson et al., 1992b). We observed that treatment with 2 μg/ml BFA for 5 min was sufficient to effect complete disappearance of endogenous GGA3 staining from both the juxtanuclear area and peripheral foci (Fig. 5, A and B). At this early time of treatment, the Golgi cisternae and TGN had not yet disrupted, suggesting that the disappearance of GGA3 staining was not due to redistribution of the Golgi complex to the ER or endo-

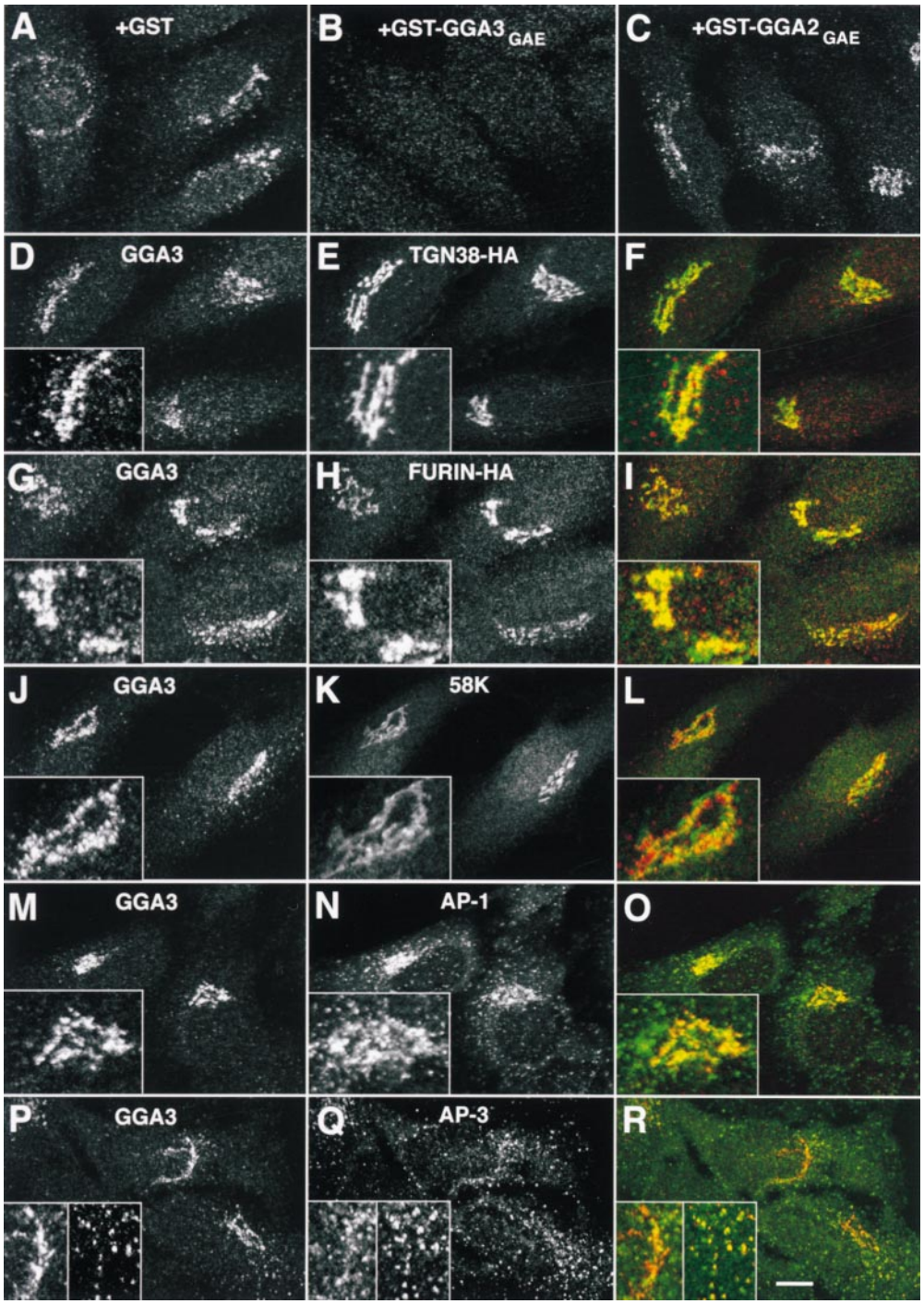

Figure 3. Intracellular localization of endogenous GGA3 analyzed by indirect immunofluorescence microscopy. A–C, HeLa cells were fixed, permeabilized, and incubated with rabbit antibody to the GAE domain of GGA3 in the presence of excess GST (A), GST-$GGA3_{GAE}$ (B), or GST-$GGA2_{GAE}$ (C) proteins. The bound antibody was revealed by staining with Cy3-conjugated donkey anti–rabbit IgG. D–R, HeLa cells transfected with HA-tagged TGN38 (D–F) or HA-tagged furin constructs (G–I), or untransfected HeLa cells (J–R) were fixed, permeabilized, and double-labeled with rabbit antibody to GGA3 followed by Cy3-conjugated donkey anti-rabbit IgG (D, G, J, M, and P; red channel), and mouse antibodies to the HA epitope (E and H), the 58K-Golgi protein (K), the γ1-adaptin subunit of AP-1 (N,100/3), or the AP-3 complex (Q, mouse polyclonal antibody to AP-3), followed by Alexa-488–conjugated donkey anti–mouse IgG (green channel). Stained cells were examined by confocal fluorescence microscopy. The third picture on each row in D–R was generated by merging of the images in the red and green channels; yellow indicates overlapping localization. Insets in D–O and the left inset in P–R show twofold magnified views of the Golgi region of the cells. The right inset in P–R shows a twofold magnified view of the peripheral cytoplasm. Bar, 10 μm.

somes, but rather to dissociation into the cytosol. Removal of BFA from the culture medium resulted in reassociation of GGA3 with both the juxtanuclear and peripheral structures (Fig. 5 C), indicating that the effects of the drug were reversible. Similar effects of BFA were observed for Myc-GGA1 and GGA2 expressed by transfection into HeLa cells (data not shown).

Another test for the involvement of ARF1 in recruitment of protein coats to membranes is the expression of dominant-negative ARF1 mutants. Overexpression of such dominant-negative mutants renders endogenous ARF1 inactive by sequestering guanine nucleotide exchange factors required for their activation (Peyroche et al., 1999); this in turn elicits dissociation of protein coats similar to that caused by BFA (Dascher and Balch, 1994; Peters et al., 1995; Ooi et al., 1998). Overexpression of dominant-negative ARF6, on the other hand, has no effects on protein coats (Peters et al., 1995; Ooi et al., 1998). We observed that overexpression of dominant-negative ARF1/T31N in HeLa cells resulted in disappearance of endogenous GGA3 from its juxtanuclear location (Fig. 5, D and E). A dominant-negative ARF5/T31N mutant had a simi-

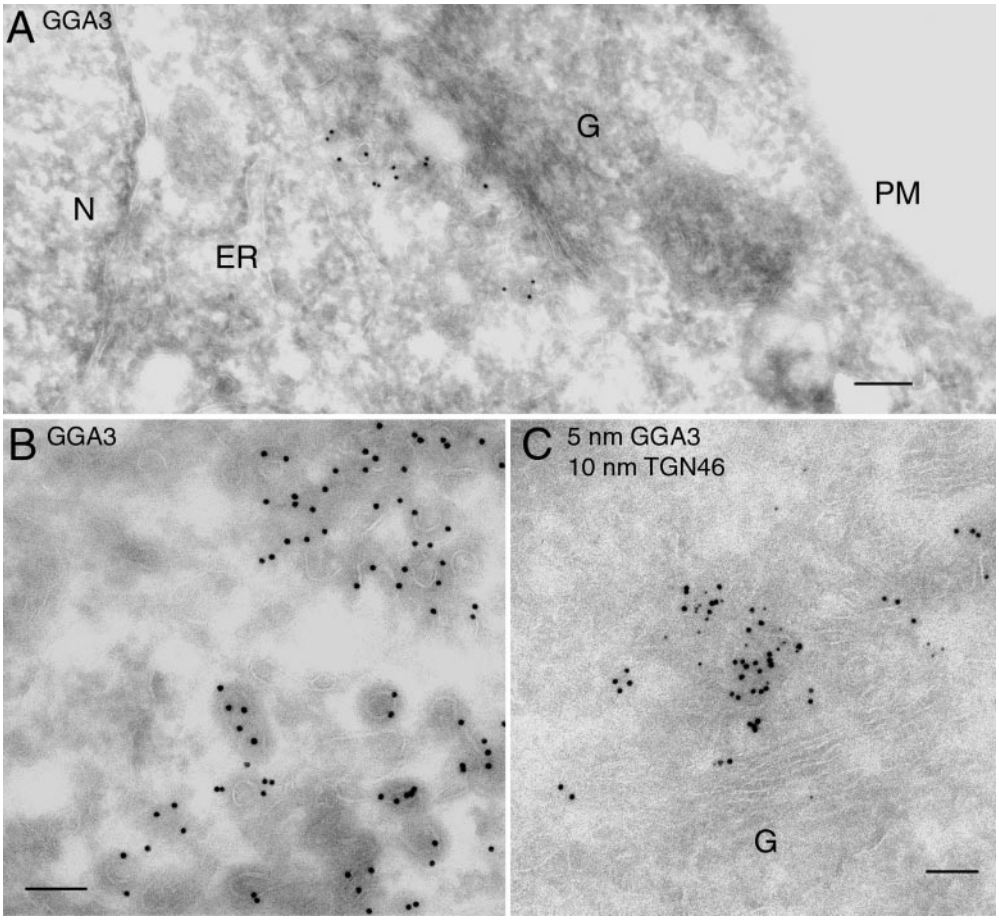

Figure 4. Ultrastructural analysis of GGA3 localization by immunoelectron microscopy. Ultrathin frozen sections of HeLa cells transfected with a GGA3 construct were immunolabeled for GGA3 (10-nm gold; A and B) or for GGA3 (5-nm gold) and TGN46 (10-nm gold; C), as described in Materials and Methods. N, nucleus; G, Golgi stack; ER, endoplasmic reticulum; PM, plasma membrane. Bars: (A) 0.2 μm; (B and C) 0.1 μm.

lar, albeit less dramatic, effect (data not shown), consistent with the reduced potency of this construct in the regulation of other protein coats (Ooi et al., 1998). Overexpression of a dominant-negative ARF6/T27N construct, on the other hand, had no effect on GGA3 association with the juxtanuclear structure (Fig. 5, F and G). Taken together, the effects of BFA and the ARF1 dominant-negative mutant suggest that association of GGA with membranes is regulated by ARF1.

Targeting to the TGN Mediated by the GAT Region

We next sought to identify the region of GGA3 responsible for targeting this protein to the TGN. Expression constructs were made by fusing the green fluorescent protein (GFP) to the VHS domain alone, the VHS domain plus GAT region, the GAT region alone, or the GAE domain, as shown in Fig. 6. The constructs were expressed by transfection into HeLa cells, and their intrinsic fluorescence used to compare their localization in moderately expressing cells relative to endogenous TGN46. We observed that the VHS (Fig. 6, A–C) or GAE (Fig. 6, J–L) domain constructs were cytosolic, whereas the VHS plus GAT (Fig. 6, D–F) or GAT region (Fig. 6, G–I) constructs colocalized with TGN46. This experiment thus demonstrated that the GAT region alone (~160 amino acids) is sufficient for targeting a reporter protein to the TGN. Treatment with BFA also caused rapid dissociation of GFP-GAT from the TGN (Fig. 6, M–O).

Dissociation of ARF-regulated Coats Induced by Overexpression of the GAT Region

In the course of the experiments described above, we noticed that a fraction of the transiently transfected cells expressing the highest levels of GFP-GAT or GFP-VHS-GAT (typically 5–10%) accumulated these proteins in the cytosol, probably due to saturation of binding sites at the Golgi complex (Fig. 7, A, C, E, and I). Strikingly, these cells exhibited dissociation of AP-1, AP-3, AP-4, and COPI, as well as endogenous GGA3, from their corresponding intracellular membranes (Fig. 7, A–F, and data not shown). In contrast, the localization of AP-2 was not affected by overexpression of any of these constructs (data not shown). Overexpression of GFP-VHS or GFP-GAE constructs did not affect the distribution of the protein coats mentioned above (see for example Fig. 7, G and H). Thus, the effects of overexpressing the GAT region (or proteins having this domain) are reminiscent of manipulations that inactivate endogenous ARF1, which suggests a possible functional relationship of the GAT region to ARF1.

We also observed that high expression levels of GFP-GAT (Fig. 7, I and J), GFP-VHS-GAT, but not GFP-VHS (data not shown), caused a redistribution of TGN46 to a more diffuse peripheral location. The nature of this location was not established.

Interaction of the GAT Region with Activated ARF1

The fact that overexpression of proteins having the GAT

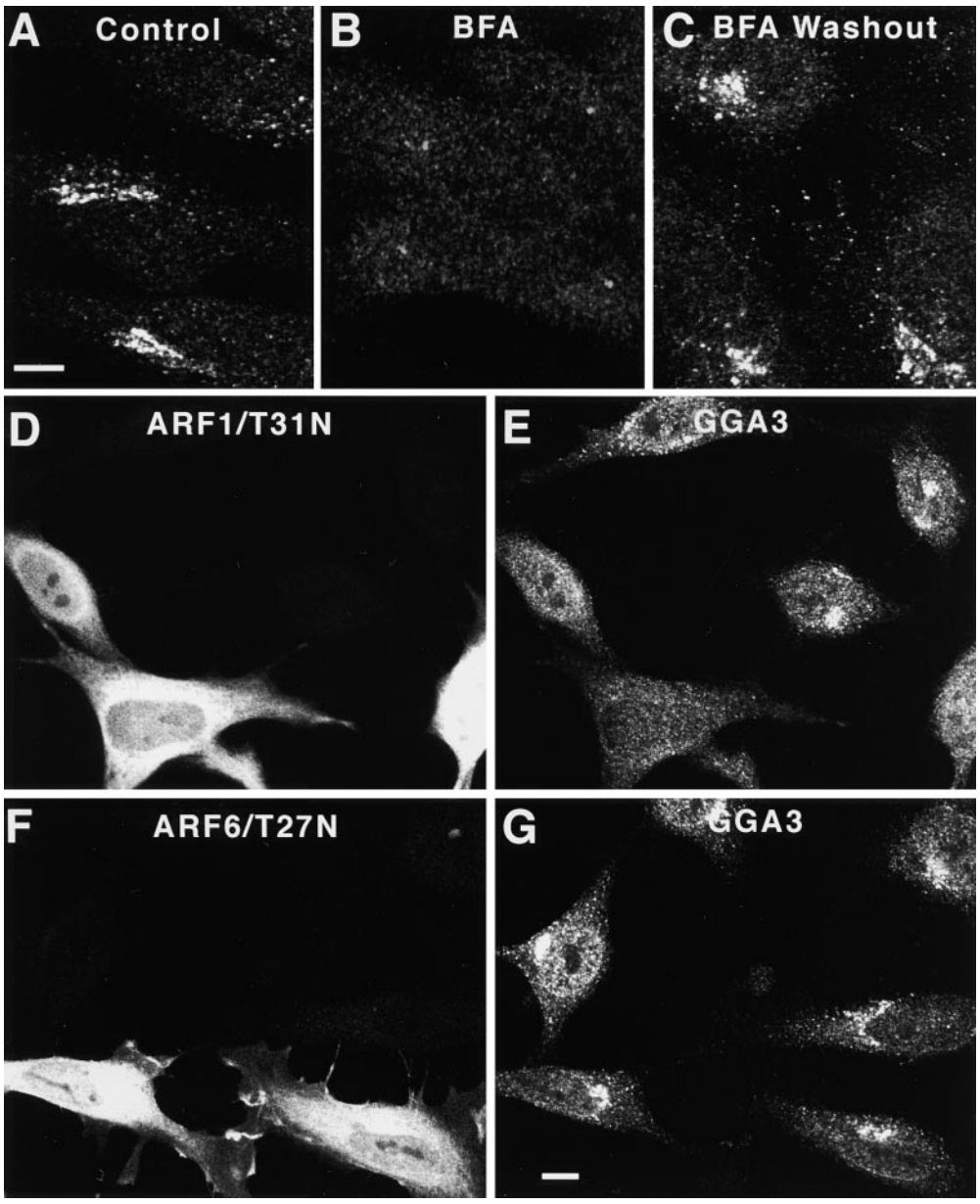

Figure 5. Effects of BFA and dominant-negative ARF mutants on the localization of endogenous GGA3 analyzed by immunofluorescence microscopy. A–C, Untreated HeLa cells (A), HeLa cells treated for 5 min at 37°C with 2 μg/ml BFA (B), or HeLa cells treated for 5 min with 2 μg/ml BFA followed by removal of the drug for 1 h at 37°C (C) were fixed, permeabilized, and incubated with rabbit antibody to GGA3, followed by Cy3-conjugated donkey anti–rabbit IgG. D–G, HeLa cells were transfected with HA-tagged ARF1/T31N (D and E) or HA-tagged ARF6/T27N (F and G). Cells were fixed, permeabilized, and double-labeled with rabbit antibody to GGA3 followed by Cy3-conjugated donkey anti–rabbit IgG (E and G), and mouse antibody to the HA epitope followed by Alexa-488–conjugated donkey anti–mouse IgG (D and F). Stained cells were examined by confocal fluorescence microscopy. Bars, 10 μm.

region caused redistribution specifically of coats regulated by ARF1 prompted us to test whether the GAT region or other portions of the GGA proteins interact directly with ARF1. To this end, we used the yeast two-hybrid system, by cotransforming a suitable yeast strain with various combinations of ARF1 and GGA-domain plasmid constructs. Interactions were assayed by complementation of histidine auxotrophy in the absence or presence of 3-amino-1,2,4-triazole (3AT) and by expression of β-galactosidase activity (Fig. 8 A). We observed that GGA3-derived VHS-GAT and GAT constructs, but not VHS or GAE constructs, interacted with the constitutively activated ARF1 mutant, ARF1/Q71L (Fig. 8 A). Interactions were strong, as growth could still be observed in the presence of 10 mM 3AT (Fig. 8 A), and β-galactosidase activity developed after just 30 min. VHS-GAT constructs derived from GGA1 and GGA2 also interacted with ARF1/Q71L (data not shown). In contrast, the inactive ARF1 mutant, ARF1/T31N, failed to interact with VHS-GAT or GAT constructs from GGA3 (Fig. 8 A), GGA1, or GGA2 (data not shown) in both the growth and β-galactosidase assays. The yeast two-hybrid assays were corroborated using in vitro binding assays in which recombinant ARF1/Q71L, or native ARF from bovine brain cytosol, were tested for interaction with GST-fusion proteins comprising different regions of GGA3 (Fig. 8 B). The GST-fusion protein having the VHS-GAT segment, but not those having the VHS or GAE regions, bound both recombinant ARF1/Q71L and bovine brain ARF upon activation with GTPγS (a nonhydrolyzable GTP analogue). In contrast, we did not observe binding in samples that had been mock-activated in the absence of GTPγS (Fig. 8 B). Furthermore, neither of two other GTP-binding proteins, Rab4 and dynamin I, interacted with the VHS-GAT segment (Fig. 8 B). Taken together, the above experiments demonstrated that the GAT region is capable of interacting with activated ARF1.

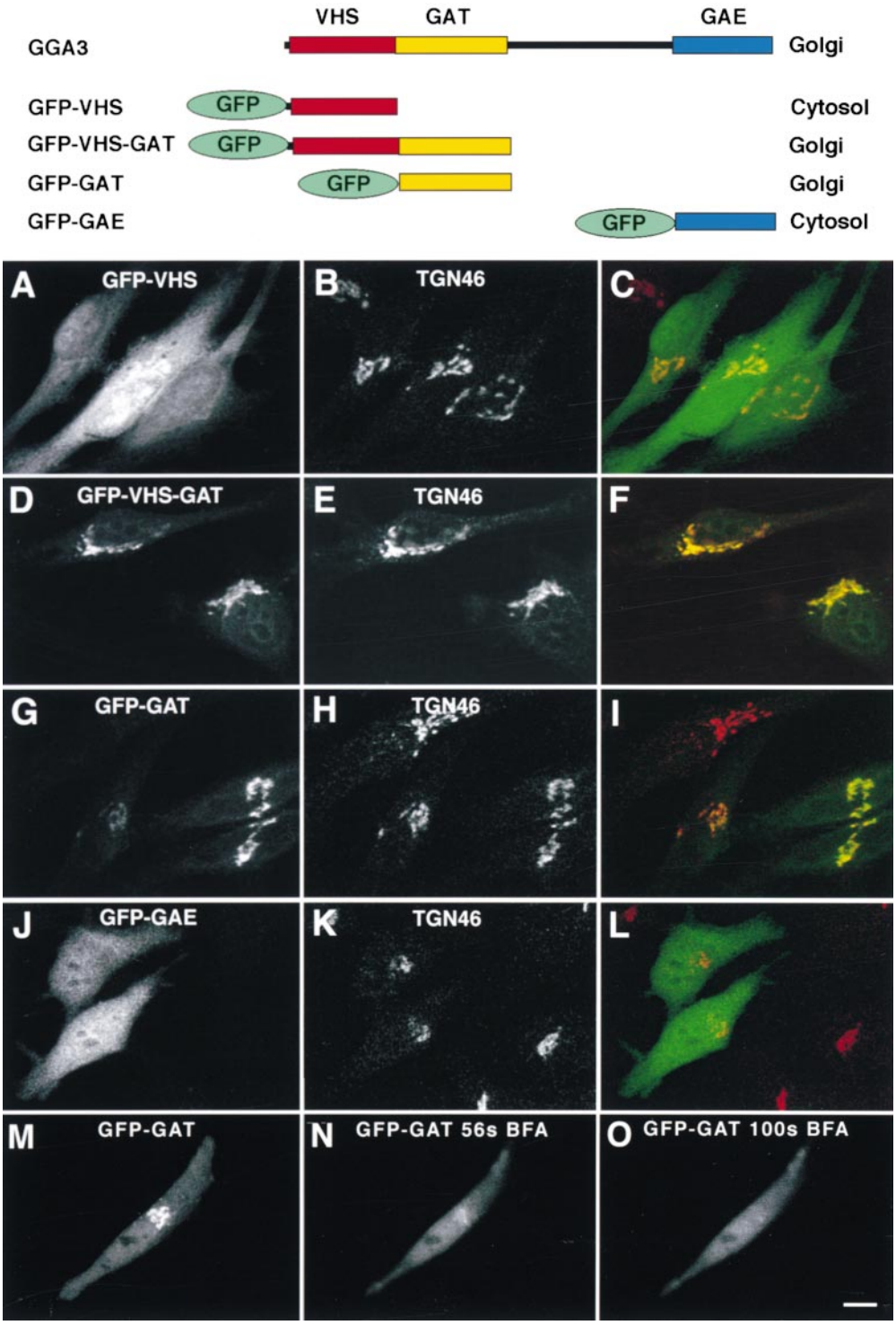

Figure 6. Intracellular localization of GFP fusion proteins containing different regions of GGA3. Top, Schematic representation of the GFP fusion proteins used in these experiments, including a summary of their localizations. A–L, Fluorescence microscopy of cells expressing GFP fusion proteins and immunostained for TGN46. HeLa cells were transfected with plasmids encoding GFP-VHS (A–C), GFP-VHS-GAT (D–F), GFP-GAT (G–I), or GFP-GAE (J–L). Transfected cells were fixed, permeabilized, and immunostained with a rabbit antibody to TGN46 followed by Cy3-conjugated donkey anti–rabbit IgG. Cells were examined by confocal fluorescence microscopy. A, D, G, and J, GFP fluorescence (green); B, E, H, and K, TGN46 (red). M–O, Live cells expressing GFP-GAT were imaged at 37°C by confocal fluorescence microscopy immediately before (M), and 56 s (N) and 100 s (O) after addition of 10 μg/ml BFA. Bar, 10 μm.

Disruption of Both Yeast GGA Genes Impairs CPY Sorting to the Vacuole

The predominant localization of the human GGAs to the TGN pointed to their possible role in sorting at this organelle. To test this hypothesis, the yeast *GGA* genes were disrupted by homologous recombination. Both single (*gga1*Δ and *gga2*Δ), as well as the double (*gga1*Δ/*gga2*Δ), mutant strains were viable and grew at rates indistinguishable from that of the wild-type parental strain at 23, 30, and 37°C (data not shown). To investigate a possible sorting defect in the mutant strains, we examined the trafficking of the vacuolar enzyme, CPY.

Immunoblot analysis revealed that the *gga1*Δ and *gga2*Δ strains contained mostly mature, 61-kD CPY, similar to the parental wild-type strain (Fig. 9 A). The *gga1*Δ/*gga2*Δ strain, on the other hand, displayed a reduced amount of mature CPY and increased amounts of larger CPY species, particularly the Golgi precursor form (p2; Fig. 9 A).

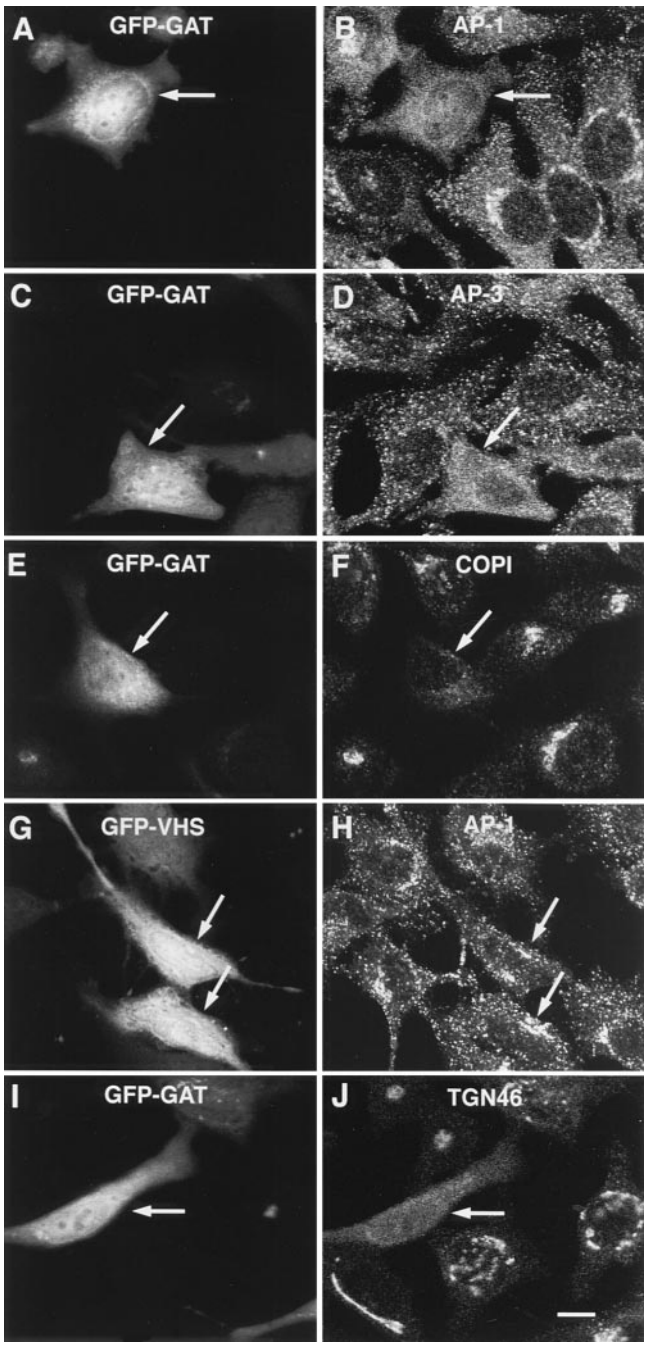

Figure 7. Effects of overexpression of GFP-GAT or GFP-VHS on protein coats and TGN46 analyzed by fluorescence microscopy. HeLa cells were transfected with plasmids encoding GFP fused to either the GAT (A–F, I and J) or VHS (G and H) regions of GGA3. Cells were fixed, permeabilized, and incubated with the 100/3 antibody to the γ1-adaptin subunit of AP-1 (B and H), the β3C1 antibody to the β3A subunit of AP-3 (D), or rabbit antibodies to the β-COP subunit of COPI (F) or TGN46 (J). Bound antibodies were revealed by staining with either Cy3-conjugated donkey anti–mouse IgG (B and H) or Cy3-conjugated donkey anti–rabbit IgG (D, F, and J). A, C, E, and I, GFP-GAT; G, GFP-VHS. Arrows point to cells that overexpress the GFP constructs. Bar, 10 μm.

Pulse–chase and immunoprecipitation analyses showed that all of the CPY was processed from the p1 and p2 precursors to the mature form within 15 min of chase in the wild-type strain (Fig. 9 B). In contrast, only ~50% of the CPY precursors were processed to the mature form, even after 30 min of chase in the *gga1*Δ/*gga2*Δ strain, with the rest accumulating as the Golgi precursor form p2 (Fig. 9 B). These analyses thus demonstrated that mutation of both *GGA* genes results in delayed processing of p2 to mature CPY (Fig. 9 B). In addition, a colony blotting assay revealed significant secretion of immunoreactive CPY in the *gga1*Δ/*gga2*Δ strain (Fig. 9 C). Thus, the delayed processing of CPY to the mature, vacuolar form was likely due to impaired transport to the vacuole and partial missorting to the periplasmic space.

Discussion

Assembly of protein coats involved in vesicle formation and cargo selection is a complex process requiring the concerted action of many structural and regulatory proteins. These proteins establish dynamic networks of low affinity interactions that cooperatively lead to the assembly of stable coats on membranes. Most proteins involved in coat assembly have a modular structure, which enables them to interact simultaneously with multiple other proteins and/or membrane lipids. The three human and two yeast members of the GGA family reported fit this description, as they are composed of at least four distinct regions referred to as VHS, GAT, linker and GAE. Despite the homology of this latter region to the ear domain of the γ1-adaptin subunit of AP-1, the GGAs represent a novel type of adaptor-related proteins that are not part of AP complexes.

The VHS domain has been previously identified in a group of proteins thought to play roles in protein trafficking and/or signal transduction (Lohi and Lehto, 1998, and references therein). Although some of these proteins have been localized to endocytic vesicles (Piper et al., 1995; Asao et al., 1997; Komada et al., 1997; Lohi et al., 1998), it is currently unclear whether the VHS domain can function as a localization determinant. In this regard, our experiments show that a GFP fusion protein containing the VHS domain of GGA3 is cytosolic, suggesting that this domain is insufficient to confer association with intracellular membranes.

Immediately adjacent to the COOH terminus of the VHS domain of the GGA proteins is a region that we call GAT. The three human GGA proteins are highly homologous in the GAT region, and also exhibit significant, albeit more limited, homology to analogous regions in the two yeast Ggaps and the human TOM1 and TOM1L1 proteins (Seroussi et al., 1999). We report here that, unlike the VHS domain, the GAT region of GGA3 alone is intrinsically capable of targeting proteins to the Golgi complex and mediating interactions with activated ARF1. It is currently unclear whether these two activities map to the same sites on the GAT region and whether the analogous regions of TOM1 and TOM1L1 have these activities. This combination of a membrane targeting function and an ability to interact with a small GTP-binding protein, however, is a characteristic of other protein modules, such as

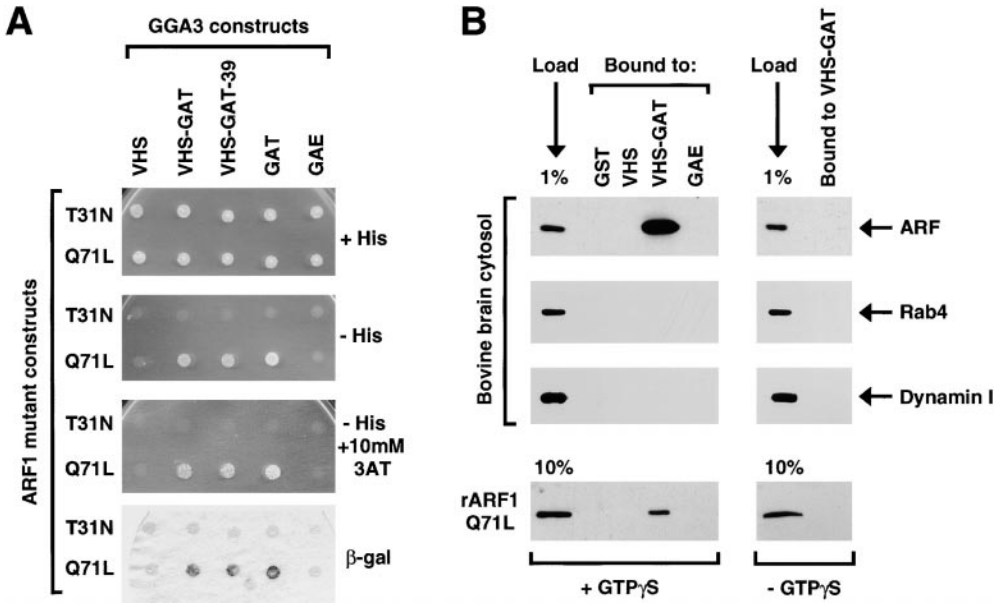

Figure 8. Binding of activated ARF1 to the GAT domain of GGA3. A, Two-hybrid assays. Yeast transformants expressing the combinations of constructs indicated in the figure were spotted onto plates lacking leucine and tryptophan, with or without histidine (+His and −His, respectively), and in the absence or presence of 10 mM 3AT. Filter β-galactosidase (β-gal) assays were performed on cells grown in the presence of histidine. Notice the growth in the absence of histidine and the positive β-galactosidase activity of transformants expressing the activated ARF1 mutant (Q71L) and the GGA3 constructs that include the GAT domain. B, In vitro binding assays. Bovine brain cytosol and recombinant ARF1/Q71L were either treated with 0.1 mM GTPγS (+GTPγS) or mock-treated (–GTPγS), and subsequently incubated with glutathione-Sepharose beads containing GST or GST-fusion proteins comprising the VHS, VHS-GAT, or GAE domains of human GGA3. Bound proteins were analyzed by immunoblotting, using the 1D9 antibody to ARF or antibodies to the Rab4 and dynamin I GTP-binding proteins. Notice the GTPγS-dependent binding of bovine brain ARF, and of recombinant ARF1/Q71L, to the GST-fusion protein bearing the VHS-GAT segment, but not the VHS or GAE regions, of GGA3.

the FYVE (Simonsen et al., 1998) and GRIP (Barr, 1999) domains.

The intervening segment between the GAT region and GAE domain of both human GGAs and yeast Ggaps is rich in proline and serine residues and has a high probability of random coils. These features suggest that this region may act as a flexible hinge that links the VHS-GAT and GAE domains of the proteins. The linker region of human GGA2 contains the sequence LIDLE, and that of yeast Gga1p the sequences LIDFD and LLDFD, all of which conform to the motif L(L,I)(D,E,N)(L,F)(D,E) implicated in binding to the clathrin terminal domain (Dell'Angelica et al., 1998). Imperfect variants of this motif are also present in the other GGA proteins. Whether any of these motifs are actually capable of mediating interactions of GGAs with clathrin will have to be investigated experimentally.

By analogy with the ear domains of the α/γ/δ/ϵ AP subunits, the GAE domain of GGAs could interact with regulatory molecules. Indeed, GST pulldown assays have shown that the GAE domains of GGAs and γ-adaptins bind a number of cytosolic proteins, some of which may be involved in coated vesicle formation (Hirst et al., 2000).

Our immunoelectron microscopy and subcellular fractionation analyses suggest that GGAs are components of protein coats that cycle between the cytosol and membranes. Moreover, the dissociation of GGA3 or GFP-GAT from membranes induced by treatment with BFA or expression of a dominant-negative ARF1, as well as the direct interaction of the GAT domain with activated ARF1, suggest that recruitment of GGAs to membranes is regulated by the ARF GTP/GDP cycle. Since the GGAs do not contain domains that are characteristic of guanine nucleotide exchange factors or GTPase activating proteins, they are most likely to function as ARF effectors. This places the GGAs in the same category as other ARF1-regulated protein coats, such as COPI, AP-1, AP-3, and AP-4. It remains to be established, however, whether GGAs are themselves structural components of novel coats, or regulators of the assembly of other coats.

Immunofluorescence and immunoelectron microscopy analyses suggest that GGA3 is mainly associated with the TGN and may therefore be involved in trafficking events at this organelle. We have also noticed faint punctate staining for GGA3 in the peripheral cytoplasm and partial colocalization of GGA3 with AP-1 and AP-3 on immunofluorescence microscopy; this suggests the existence of an additional pool of GGA3 associated with peripheral (perhaps endosomal) structures. The GFP-GAT chimera also shows good colocalization with TGN markers. However, its pattern of staining is continuous rather than punctate. A possible explanation for this observation is that GFP-GAT is properly targeted to the TGN, but lacks the ability to concentrate in coated vesicles and buds.

Overexpression of GFP-GAT, but not GFP fusion proteins having other domains of GGA3, causes dissociation of ARF1-regulated coats from membranes. This correlates well with the ability of the GAT region to interact with activated ARF1. This could mean that GGAs play roles in the ARF1-mediated deposition of protein coats onto membranes. A more likely explanation, however, is that overexpression of GFP-GAT either sequesters activated ARF1 or blocks a common effector binding site within the ARF1 molecule, thus preventing recruitment of other coats to membranes.

The existence of two GGA homologues in yeast has allowed us to assess the function of these proteins in vivo.

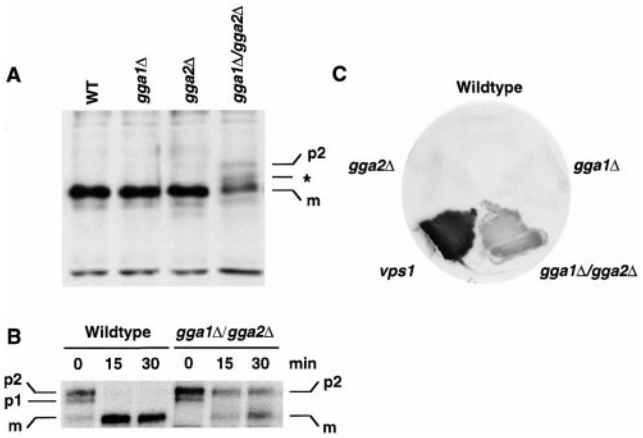

Figure 9. Effects of disruption of yeast *GGA* genes on CPY processing and secretion. A, Immunoblot analysis of CPY in whole-cell lysates of wild-type, *gga1*Δ, *gga2*Δ, and *gga1*Δ/*gga2*Δ strains. The positions of the p2 and m forms of CPY are indicated. The asterisk indicates an unidentified intermediate species. B, Wild-type and *gga1*Δ/*gga2*Δ strains were pulse-labeled with [^{35}S]methionine for 10 min at 30°C and then chased for 0, 15, or 30 min at 30°C. CPY was isolated by immunoprecipitation and analyzed by SDS-PAGE and fluorography. The positions of the p1, p2, and m forms of CPY are indicated. C, Colony blotting analysis of CPY secretion. Nitrocellulose replicas of streaks of the strains mentioned in A and of a *vps1* mutant strain (positive control) were probed with anti-CPY antiserum to reveal secreted CPY.

Double-mutants of genes encoding these proteins displayed delayed processing of CPY from a Golgi to a vacuolar form. In addition, we observed secretion of immunoreactive CPY into the periplasmic space. These observations are consistent with impairment of transport to the vacuole, a phenotype characteristic of *vps* mutants (Horazdovsky et al., 1995; Conibear and Stevens, 1998). Mutation of either of the two yeast *GGA* genes individually had little or no effect on CPY processing and secretion, suggesting that both gene products fulfill redundant functions. Perhaps this is also the explanation for the existence of three GGAs in humans.

In conclusion, our studies of human and yeast GGAs suggest that these proteins are components of coats associated mainly with the TGN in an ARF1-dependent manner, and involved in protein trafficking at this organelle.

We thank Xiaolin Zhu for excellent technical assistance, John Presley for help with confocal microscopy, Paul Randazzo, Chean Eng Ooi, Victor Hsu, Vas Ponnambalam, Tom Stevens, and Carol Woolford for generous gifts of reagents, and Julie Donaldson, Paul Randazzo and Margaret S. Robinson for helpful discussions and comments on the manuscript.

R. Puertollano was supported by a postdoctoral fellowship from the Fundación Ramón Areces and C. Mullins by a National Research Council Associateship.

Submitted: 5 January 2000
Revised: 15 February 2000
Accepted: 22 February 2000

References

Asao, H., Y. Sasaki, T. Arita, N. Tanaka, K. Endo, H. Kasai, T. Takeshita, Y. Endo, T. Fujita, and K. Sugamura. 1997. Hrs is associated with STAM, a signal-transducing adaptor molecule. Its suppressive effect on cytokine-induced cell growth. *J. Biol. Chem.* 272:32785–32791.

Barr, F.A. 1999. A novel Rab6-interacting domain defines a family of Golgi-targeted coiled-coil proteins. *Curr. Biol.* 9:381–384.

Berben, G., J. Dumont, V. Gilliquet, P.A. Bolle, and F. Hilger. 1991. The YDp plasmids: a uniform set of vectors bearing versatile gene disruption cassettes for *Saccharomyces cerevisiae. Yeast.* 7:475–477.

Boman, A.L., and R.A. Kahn. 1995. Arf proteins: the membrane traffic police? *Trends Biochem. Sci.* 20:147–150.

Boman, A.L., C.-J. Zhang, X. Zhu, and R.A. Kahn. 2000. A family of Arf effectors that can alter membrane transport through the trans-Golgi. *Mol. Biol. Cell.* In press.

Bonifacino, J.S., and E.C. Dell'Angelica. 1999. Molecular bases for the recognition of tyrosine-based sorting signals. *J. Cell Biol.* 145:923–926.

Conibear, E., and T.H. Stevens. 1998. Multiple sorting pathways between the late Golgi and the vacuole in yeast. *Biochim. Biophys. Acta.* 1404:211–230.

Dascher, C., and W.E. Balch. 1994. Dominant inhibitory mutants of ARF1 block endoplasmic reticulum to Golgi transport and trigger disassembly of the Golgi apparatus. *J. Biol. Chem.* 269:1437–1448.

Dell'Angelica, E.C., H. Ohno, C.E. Ooi, E. Rabinovich, K.W. Roche, and J.S. Bonifacino. 1997. AP-3: an adaptor-like protein complex with ubiquitous expression. *EMBO (Eur. Mol. Biol. Organ.) J.* 15:917–928.

Dell'Angelica, E.C., J. Klumperman, W. Stoorvogel, and J.S. Bonifacino. 1998. Association of the AP-3 adaptor complex with clathrin. *Science.* 280:431–434.

Dell'Angelica, E.C., C. Mullins, and J.S. Bonifacino. 1999a. AP-4, a novel protein complex related to clathrin adaptors. *J. Biol. Chem.* 274:7278–7285.

Dell'Angelica, E.C., V. Shotelersuk, R.C. Aguilar, W.A. Gahl, and J.S. Bonifacino. 1999b. Altered trafficking of lysosomal proteins in Hermansky-Pudlak syndrome due to mutations in the β3A subunit of the AP-3 adaptor. *Mol. Cell.* 3:11–21.

Dell'Angelica, E.C., R.C. Aguilar, N. Wolins, S. Hazelwood, W.A. Gahl, and J.S. Bonifacino. 2000. Molecular characterization of the protein encoded by the Hermansky-Pudlak syndrome type 1 gene. *J. Biol. Chem.* 275:1300–1308.

Donaldson, J.G., D. Cassel, R.A. Kahn, and R.D. Klausner. 1992a. ADP-ribosylation factor, a small GTP-binding protein, is required for binding of the coatomer protein β-COP to Golgi membranes. *Proc. Natl. Acad. Sci. USA.* 89:6408–6412.

Donaldson, J.G., D. Finazzi, and R.D. Klausner. 1992b. Brefeldin A inhibits Golgi membrane-catalysed exchange of guanine nucleotide onto ARF protein. *Nature.* 360:350–352.

Faundez, V., J.T. Horng, and R.B. Kelly. 1998. A function for the AP3 coat complex in synaptic vesicle formation from endosomes. *Cell.* 93:423–432.

Hampton, R.Y., and J. Rine. 1994. Regulated degradation of HMG-CoA reductase, an integral membrane protein of the endoplasmic reticulum, in yeast. *J. Cell Biol.* 125:299–312.

Herman, P.K., and S.D. Emr. 1990. Characterization of VPS34, a gene required for vacuolar protein sorting and vacuole segregation in *Saccharomyces cerevisiae. Mol. Cell. Biol.* 10:6742–6754.

Heuser, J.E., and J. Keen. 1988. Deep-etch visualization of proteins involved in clathrin assembly. *J. Cell Biol.* 107:877–886.

Hirst, J., and M.S. Robinson. 1998. Clathrin and adaptors. *Biochim. Biophys. Acta.* 1404:173–193.

Hirst, J., N.A. Bright, B. Rous, and M.S. Robinson. 1999. Characterization of a fourth adaptor-related protein complex. *Mol. Biol. Cell.* 10:2787–2802.

Hirst, J., W.W.Y. Lui, N.A. Bright, N. Totty, M.N.J. Seaman, and M.S. Robinson. 2000. A family of proteins with γ-adaptin and VHS domains that facilitate trafficking between the trans-Golgi network and the vacuole/lysosome. *J. Cell. Biol.* 149:67–79.

Horazdovsky, B.F., D.B. DeWald, and S.D. Emr. 1995. Protein transport to the yeast vacuole. *Curr. Opin. Cell Biol.* 7:544–551.

Kikuno, R., T. Nagase, K.-I. Ishikawa, M. Kirosawa, N. Miyajima, A. Tanaka, H. Kotani, N. Nomura, and O. Ohara. 1999. Prediction of the coding sequences of unidentified human genes. XIV. The complete sequences of 100 new cDNA clones from brain which code for large proteins *in vitro. DNA Res.* 6:197–205.

Kirchhausen, T. 1999. Adaptors for clathrin-mediated traffic. *Annu. Rev. Cell Dev. Biol.* 15:705–732.

Kirchhausen, T., J.S. Bonifacino, and H. Riezman. 1997. Linking cargo to vesicle formation: receptor tail interactions with coat proteins. *Curr. Opin. Cell Biol.* 9:488–495.

Komada, M., R. Masaki, A. Yamamoto, and N. Kitamura. 1997. Hrs, a tyrosine kinase substrate with a conserved double zinc finger domain, is localized to the cytoplasmic surface of early endosomes. *J. Biol. Chem.* 272:20538–20544.

Ktistakis, N.T., H.A. Brown, M.G. Waters, P.C. Sternweis, and M.G. Roth. 1996. Evidence that phospholipase D mediates ADP ribosylation factor-dependent formation of Golgi-coated vesicles. *J. Cell Biol.* 134:295–306.

Lewin, D.A., D. Sheff, C.E. Ooi, J.A. Whitney, E. Yamamoto, L.M. Chicione, P. Webster, J.S. Bonifacino, and I. Mellman. 1998. Cloning, expression, and localization of a novel γ-adaptin-like molecule. *FEBS Lett.* 435:263–268.

Liang, J.O., and S. Kornfeld. 1997. Comparative activity of ADP-ribosylation factor family members in the early steps of coated vesicle formation on rat liver Golgi membranes. *J. Biol. Chem.* 272:4141–4148.

Lippincott-Schwartz, J., N.B. Cole, and J.G. Donaldson. 1998. Building a secretory apparatus: role of ARF1/COPI in Golgi biogenesis and maintenance. *Histochem. Cell Biol.* 109:449–462.

Loftus, B.J., U.J. Kim, V.P. Sneddon, F. Kalush, R. Brandon, J. Fuhrmann, T.

Mason, M.L. Crosby, M. Barnstead, L. Cronin, et al. 1999. Genome duplications and other features in 12 Mb of DNA sequence from human chromosome 16p and16q. *Genomics*. 60:295–308.

Lohi, O., and V.P. Lehto. 1998. VHS domain marks a group of proteins involved in endocytosis and vesicular trafficking. *FEBS Lett.* 440:255–257.

Lohi, O., A. Poussu, J. Merilainen, S. Kellokumpu, V.M. Wasenius, and V.P. Lehto. 1998. EAST, an epidermal growth factor receptor- and Eps15-associated protein with Src homology 3 and tyrosine-based activation motif domains. *J. Biol. Chem*. 273:21408–21415.

Mellman, I. 1996. Endocytosis and molecular sorting. *Annual Rev. Cell Dev. Biol.* 12:575–625.

Moss, J., and M. Vaughan. 1998. Molecules in the ARF orbit. *J. Biol. Chem*. 273:21431–21434.

Mullins, C., Y. Lu, A. Campbell, H. Fang, and N. Green. 1995. A mutation affecting signal peptidase inhibits degradation of an abnormal membrane protein in *Saccharomyces cerevisiae. J. Biol. Chem*. 270:17139–17147.

Nagase, T., N. Seki, A. Tanaka, K.-I. Ishikawa, and N. Nomura. 1995. Prediction of the coding sequences of unidentified human genes. IV. The coding sequences of 40 new genes (KIAA0121-KIAA0160) deduced by analysis of cDNA clones from human cell line KG-1. *DNA Res.* 2:167–174.

Ooi, C.E., E.C. Dell'Angelica, and J.S. Bonifacino. 1998. ADP-ribosylation factor 1 (ARF1) regulates recruitment of the AP-3 adaptor complex to membranes. *J. Cell Biol.* 142:391–402.

Palmer, D.J., J.B. Helms, C.J. Beckers, L. Orci, and J.E. Rothman. 1993. Binding of coatomer to Golgi membranes requires ADP-ribosylation factor. *J. Biol. Chem*. 268:12083–12089.

Peters, P.J., V.W. Hsu, C.E. Ooi, D. Finazzi, S.B. Teal, V. Oorschot, J.G. Donaldson, and R.D. Klausner. 1995. Overexpression of wild-type and mutant ARF1 and ARF6: distinct perturbations of nonoverlapping membrane compartments. *J. Cell Biol.* 128:1003–1017.

Peyroche, A., B. Antonny, S. Robineau, J. Acker, J. Cherfils, and C.L. Jackson. 1999. Brefeldin A acts to stabilize an abortive ARF-GDP-Sec7 domain protein complex: involvement of specific residues of the Sec7 domain. *Mol. Cell*. 3:275–285.

Piper, R.C., A.A. Cooper, H. Yang, and T.H. Stevens. 1995. VPS27 controls vacuolar and endocytic traffic through a prevacuolar compartment in *Saccharomyces cerevisiae. J. Cell Biol.* 131:603–617.

Radhakrishna, H., R.D. Klausner, and J.G. Donaldson. 1996. Aluminum fluoride stimulates surface protrusions in cells overexpressing the ARF6 GTPase. *J. Cell Biol.* 134:935–947.

Roberts, C.J., C.K. Raymond, C.T. Yamashiro, and T.H. Stevens. 1991. Methods for studying the yeast vacuole. *Methods Enzymol.* 194:644–661.

Robinson, M.S. 1990. Cloning and expression of γ-adaptin, a component of clathrin-coated vesicles associated with the Golgi apparatus. *J. Cell Biol.* 111:2319–2326.

Robinson, M.S., and T.E. Kreis. 1992. Recruitment of coat proteins onto Golgi membranes in intact and permeabilized cells: effects of brefeldin A and G protein activators. *Cell*. 69:129–138.

Rothman, J.E., and F.T. Wieland. 1996. Protein sorting by transport vesicles. *Science*. 272:227–234.

Schekman, R., and L. Orci. 1996. Coat proteins and vesicle budding. *Science*. 271:1526–1533.

Seroussi, E., D. Kedra, M.K. Alimova, A.C.S. Nordqvist, I. Fransson, J.F. Jacobs, Y. Fu, H.Q. Pan, B.A. Roe, S. Imreh, and J.P. Dumanski. 1999. TOM1 genes map to human chromosome 22q13.1 and mouse chromosome 8C1 and encode proteins similar to the endosomal proteins HGS and STAM. *Genomics*. 57:380–388.

Simonsen, A., R. Lippe, S. Christoforidis, J.M. Gaullier, A. Brech, J. Callaghan, B.H. Toh, C. Murphy, M. Zerial, and H. Stenmark. 1998. EEA1 links PI(3)K function to Rab5 regulation of endosome fusion. *Nature*. 394:494–498.

Slot, J.W., and H.J. Geuze. 1983. The use of protein A-colloidal gold (PAG) complexes as immunolabels in ultrathin frozen sections. *In* Immunocytochemistry. A.C. Cuello, editor. J. Wiley & Sons, Chichester. 323–346.

Stamnes, M.A., and J.E. Rothman. 1993. The binding of AP-1 clathrin adaptor particles to Golgi membranes requires ADP-ribosylation factor, a small GTP-binding protein. *Cell*. 73:999–1005.

Takatsu, H., S. Michinari, H.Y. Shin, K. Murakami, and K. Nakayama. 1998. Identification and characterization of novel clathrin adaptor-related proteins. *J. Biol. Chem*. 273:24693–24700.

Traub, L.M., J.A. Ostrom, and S. Kornfeld. 1993. Biochemical dissection of AP-1 recruitment onto Golgi membranes. *J. Cell Biol.* 123:561–573.

Wieland, F., and C. Harter. 1999. Mechanisms of vesicle formation: insights from the COP system. *Curr. Opin. Cell Biol.* 11:440–446.

Zhao, L., J.B. Helms, B. Brugger, C. Harter, B. Martoglio, R. Graf, J. Brunner, and F.T. Wieland. 1997. Direct and GTP-dependent interaction of ADP ribosylation factor 1 with coatomer subunit beta. *Proc. Natl. Acad. Sci. USA*. 94:4418–4423.